Available online at www.sciencedirect.com
SCIENCE DIRECT
Thermochimica Acta 440 (2006) 23–30
thermochimica acta
www.elsevier.com/locate/tca

Thermogravimetric analysis and kinetics modeling of isothermal carbonization of olive wood in inert atmosphere

Najla Grioui [a], Kamel Halouani [a,*], André Zoulalian [b], Foued Halouani [c]

[a] *Micro-Electro-Thermal Systems – Industrial Energy Systems Group (METS-IESG), Institut Préparatoire aux Etudes d'Ingénieurs de Sfax (IPEIS), B.P. 805, 3000 Sfax, Tunisie*

[b] *Laboratoire d'Etudes et de Recherches sur le Matériau Bois (LERMAB), Université Henri Point Carré Nancy 1 (UHP), B.P. 239, 54506 Vandoeuvre lès Nancy Cedex, France*

[c] *Ecole Nationale d'Ingénieurs de Sfax (ENIS), B.P. 3038, Sfax, Tunisie*

Received 3 May 2005; received in revised form 9 September 2005; accepted 30 September 2005
Available online 8 November 2005

Abstract

The kinetics of olive wood carbonization is investigated by means of isothermal thermogravimetric analysis method. Measurements were carried out in a thermobalance for different fixed temperatures between 498 and 648 K. A two-stage semi-global kinetic model consisting of four sequential steps was proposed to derive kinetic parameters. The olive wood is classified in three pseudo-components. For the first two, similar thermal degradation mechanisms take place in a single reaction step. For the third, the thermal degradation takes place in two consecutive steps. The isothermal conditions allow the kinetic constants (activation energy and pre-exponential factors) to be estimated by means of the analytical solution of the mass conservation equations. An overall good agreement was obtained with activation energy values available in the literature.

Keywords: Carbonization; Olive wood; Kinetic parameters; TGA; Modeling

1. Introduction

Biomass, especially wood, has traditionally been an important source of energy particularly attractive nowadays because of its inherent nature of being environmentally friendly and renewable. Wood has also been considered as a potential feedstock for gasification to produce a mixture of H_2 and CO (syngas). In this process, the wood is converted into char as an intermediate product which is subsequently or simultaneously gasified. The wood carbonization in which the high yield charcoal is the principal product is effectively an initial stage in any gasification process. It is characterized by a slow heating rate, a relatively low temperature (600–700 K) and a long residence time. Indeed, the mechanism of wood carbonization shows the presence of several decomposition phases when the temperature increases. A wood drying phase with elimination of some volatile compounds takes place at temperatures lower than 473 K. For temperature range of 473–553 K, hemicelluloses are converted essentially into gases and acetic acid. This step corresponds to the wood roasting. Above 553 K, the lignin and cellulose decompose to give three products: gas, tar and char. Therefore, the knowledge of the kinetic schemes of the wood carbonization is essential. Particularly, kinetic analyses of wood carbonization, also called low temperature pyrolysis, under isothermal conditions have been carried out by several authors to represent the kinetic schemes of this process [1–8]. The simplest treatment describes the process by means of a one-step global reaction for degradation in which the activation energies vary toughly between 60 and 170 kJ mol^{-1} [1–4]. These models are not applicable for simulating wood carbonization because they assume a constant ratio of the charcoal to volatiles yield [9]. A one-step multi-reaction kinetic mechanism of beech wood was described by [5] as a two-stage temperature process in the range of 523–673 K. Two sets of kinetic parameters (activation energies of 17–115 kJ mol^{-1}) were needed depending on a limit temperature of 603 K. This kinetic scheme cannot be extended to systems different from the one on which it is based [9]. Multistage, semi-global models are developed to describe the kinetic of isothermal wood degra-

* Corresponding author. Tel.: +216 98 954 415; fax: +216 74 246 347.
E-mail addresses: Najla.Grioui@fss.rnu.tn (N. Grioui), Kamel.Halouani@ipeis.rnu.tn (K. Halouani), Andre.Zoulalian@lermab.uhp-nancy.fr (A. Zoulalian), Foued.Halouani@enis.rnu.tn (F. Halouani).

0040-6031/$ – see front matter © 2005 Elsevier B.V. All rights reserved.
doi:10.1016/j.tca.2005.09.018

Table 1
Elementary composition of Tunisian olive wood

Elementary composition	Mass fraction (%)
Carbon	45.08
Hydrogen	6.21
Nitrogen	0.4
Oxygen	45.39
Sulphur	Inferior to 0.3

dation [6–8]. For carbonization techniques where the product gases energy is recycled in the process [10], models of this type can be successfully applied to simulate thermal conversion since they include the description of the primary degradation of the virgin wood and the secondary degradation of the primary pyrolysis products. The large differences between reaction schemes and kinetic constant values proposed by previous authors show that further analysis is needed to study the multi-stage thermal degradation kinetics of wood under isothermal conditions.

The main objective of this study is to propose a two-stage, semi-global kinetic model of olive wood carbonization. Isothermal weight loss curves of olive wood, measured in an inert atmosphere for a temperature range of 498–623 K, are used to elaborate a reaction mechanisms scheme. A comparison is also made between the estimated activation energy values and those available in the literature corresponding to isothermal carbonization conditions.

2. Experimental study

2.1. Material specification

A hard olive wood, from Sfax in Tunisia, is used as raw material in all experiments. It was crushed by a robot and the obtained powder was sieved through two sieves. The particle size of the sieved powder was between 0.5 and 1 mm. Table 1 shows the obtained results of the olive wood elementary analysis realized in the Analysis Central Service of CNRS in France. By neglecting the sulphur and nitrogen fractions in the above analysis data, the empirical formula of the used wood can be represented by: $CH_{1.67}O_{0.75}$.

2.2. Apparatus description

A Setaram thermobalance apparatus is used for the thermogravimetric analysis. This apparatus records the different data concerning the evolution of the temperature and the mass loss. The thermobalance consists of three main parts:

- a controller which allows the transfer of the experimental data (mass, temperature) to a computer which records and treats them by Setsys software (e.g. DTG),
- an oven composed of an electrical resistance in graphite and a double envelope cooled by a circulation of water in order to control the heat flow and then the temperature. A PDI regulator allows to vary the rate of temperature change between 0.2 and 50 K min^{-1},
- a micro-balance, based on a compensation permitting to measure the mass of the sample placed in a basket of 5 cm^3 volume, continuously balanced and thus maintained at a fixed position during the experiment. This allows to avoid eventual intra-particle temperature gradients in isothermal conditions in the oven. The maximal mass variation is 200 mg and the mass measurement precision is 0.4 μg. The oven temperature is adjustable with a precision of 0.1 K and can reach a maximum of 1473 K. In order to establish an inert atmosphere during all experiments, a controlled argon flow fixed to 7.2 l h^{-1} at 273 K and 1 atm, sweeps the measurement cell that is purged for 20 min before starting the heating program.

2.3. Experimental methodology

The initial mass of olive wood powder in the basket is about 170 mg. The experiments start with a drying phase during which the temperature is raised from room temperature to 423 K at a heating rate of 20 K min^{-1} with a holding time of 20 min. Then, the same heating rate is applied to the oven until reaching the fixed studied temperature (pre-heated phase). This methodology is followed to reach the isothermal stage in the pre-heated wooden powder without any intra-particle gradients and in order to shorten the first thermal dynamic stage [6]. The subsequent thermal decomposition is carried out in isothermal conditions during 5 h. The same experiment is repeated for seven fixed temperatures (T = 498, 523, 548, 573, 598, 623 and 648 K). Measurements of the mass of the wooden powder are taken in a fixed position during 5 h at each temperature level. In these conditions, the diffusion time is always inferior than the reaction time. Indeed, for a wood particle of e = 0.5 mm thickness and a diffusion coefficient D between 10^{-7} and 10^{-8} m^2 s^{-1}, the diffusion time $\tau = e^2/D$ is respectively equal to 2.5 and 25 s. This time is always very small compared to the reaction time which exceeds 500 s in all the studied cases. The temperature and the concentration gradients are consequently negligible in the basket which can be assumed to have a uniform temperature and concentration.

2.4. Measurements

The residual weight curves of the olive wood, for the seven studied temperatures T = 498, 523, 548, 573, 598, 623 and 648 K, are plotted in Fig. 1. In all the experiments, the values of the total mass used are those which correspond to the fixed temperatures. In fact, to separate the mass loss during the dynamic stage (non-isothermal) of decomposition from that of the isothermal stage, particularly for higher temperatures (598, 623 and 648 K), the relative values of total mass before reaching the fixed temperature are not taken into account in the estimation of the kinetic parameters. Only the start time at the beginning of the transformation is obtained by extrapolation of the mass values corresponding to the fixed temperature. This time of origin is estimated with a rather good accuracy for the majority of the studied temperatures by an exponential extrapolation at the beginning of the experimental curves.

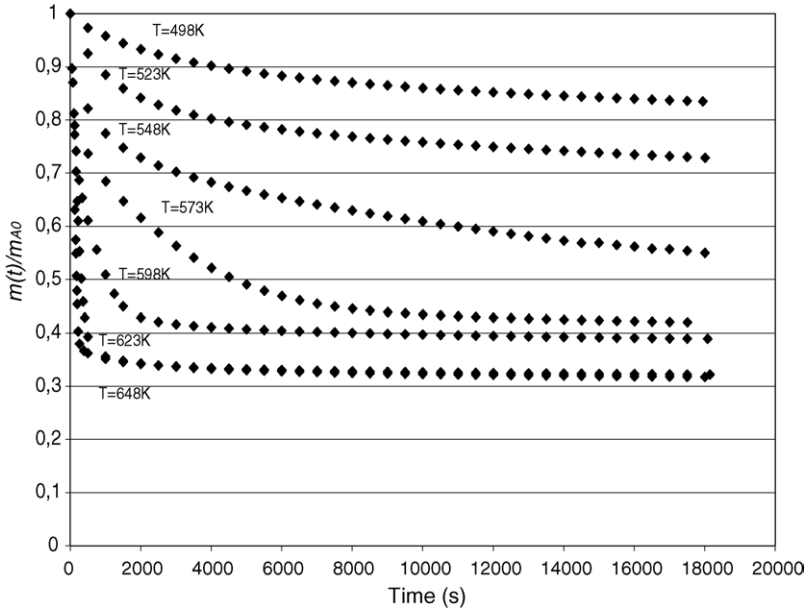

Fig. 1. Experimental mass loss curves of olive wood for the different studied temperatures.

The residual mass curves presented in Fig. 1 show that the rate of the kinetics degradation process increases with the temperature. At high temperatures (598, 623 and 648 K), a very fast mass loss stage is observed after which the mass loss $m(t)/m_{A_0}$ becomes very low. This rate becomes almost equal to zero for temperatures above 648 K. The residual mass obtained at 648 K represents 32% of the mass of the initial dried sample.

3. Kinetic modeling

Several kinetic models of wood pyrolysis [7,11–15] suggest to divide the wood into two or three parts. The models where these three parts correspond to the three main components of wood (hemicelluloses, cellulose, lignin) are not satisfactory because the thermal degradation behavior of wood has been postulated to reflect the sum of the thermal response of its three main components; inorganic components catalyze the conversion process in an unpredictable variety of ways [9,16].

In Fig. 2 we have examined experimentally the evolution of the mass loss rate of the olive wood during carbonization between 298 and 1173 K, with a slow heating rate (1.5 K min^{-1}) to avoid spatial gradients of temperature. This figure describes the thermal degradation behavior of the olive wood with increasing temperature and confirms the presence of three peaks in wood decomposition: between 353 and 423 K, the loss of mass is due to the drying phase. From 453 K, the wood decomposition starts by a first peak at 490 K. Then, a second peak appears at 543 K and finally, a third important peak appears at the temperature of about 600 K. This decomposition continues with a low rate for the higher temperatures. At 723 K, the rate of

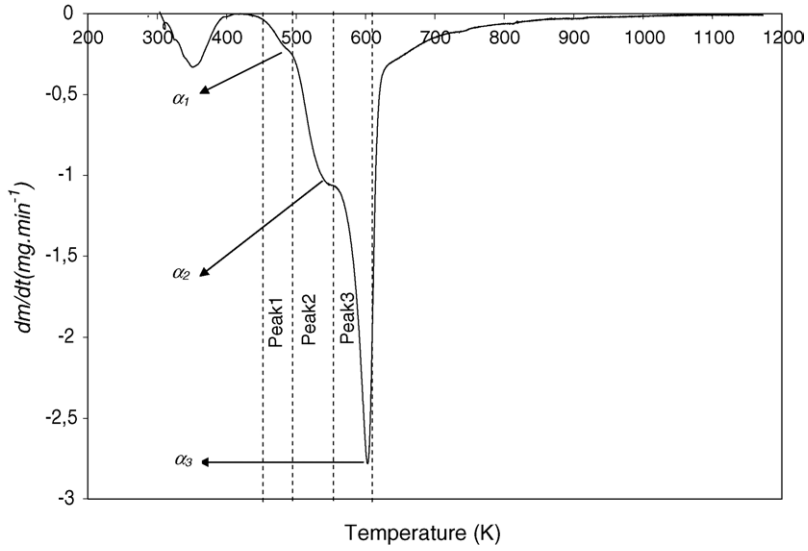

Fig. 2. Evolution of the mass loss rate of the olive wood for a temperature range of 293–1173 K.

decomposition is very low and becomes negligible at 923 K. The temperature values where the three peaks are observed in this experiment do not correspond necessarily to the decomposition temperature of the three principal components of the wood: hemicelluloses, cellulose and lignin, separately.

Based on experimental results and the wood carbonization mechanisms mentioned above, we propose to develop a two-stage, semi-global multi-reaction kinetic model of olive wood carbonization. In our model, the wood is subdivided into three pseudo-components A_1, A_2, A_3; each of them corresponds to a specific kinetic law and a mass fraction α_1, α_2 and $\alpha_3 = 1 - \alpha_1 - \alpha_2$, respectively. At low temperature ($T \leq 523\,K$), only the degradation of A_1 prevails and the product is gaseous. In fact, this level of temperature (490 K) corresponds to the elimination of some volatile wood compounds during carbonization. At high temperature, the degradation of pseudo-components A_1 and A_2 is complete and for A_3, the transformation includes two reaction steps in which the product of the first step (B) is converted into charcoal (C_3) and gases (G_4) in the second step. Indeed, for high temperatures, it can be seen from Fig. 1 that after a very fast mass loss stage, there is a very weak variation of the mass as function of the time. This abrupt change in the evolution of the mass loss is necessarily related to the presence of two consecutive or parallel stages of wood decomposition. The proposed kinetic scheme is as follows:

$$A_1\ (\text{1st pseudo component of olive wood}) \rightarrow G_1\ (\text{gas}) \quad (1)$$

$$A_2\ (\text{2nd pseudo component of olive wood}) \rightarrow \gamma_2 C_2\ (\text{charcoal}) + G_2\ (\text{gas}) \quad (2)$$

$$A_3\ (\text{3rd pseudo component of olive wood}) \rightarrow \beta B\ (\text{intermediate solid}) + G_3\ (\text{gas}) \quad (3)$$

$$B\ (\text{intermediate solid}) \rightarrow \gamma_3 C_3\ (\text{charcoal}) + G_4\ (\text{gas}) \quad (4)$$

The two first pseudo-components A_1 and A_2 degrade in a single stage reaction by giving gas products (G_1) and (G_2), respectively, and a non-degradable solid residue "charcoal" (C_2). For A_3 the thermal degradation takes place in two consecutive reaction stages. The first stage leads to an intermediate product (B) comparable to a solid (large hydrocarbon molecule) and gases (G_3). In the second stage the intermediate product (B) is transformed into a non-degradable solid "charcoal" (C_3) and gas products (G_4). The constituent B is not really a volatile intermediate product which can be degraded but its degradation rate is relatively low compared to the ones of the pseudo-components A_1, A_2 and A_3. The mass fractions (β) of the intermediate product (B) and those of the non-degradable solid "charcoal" (γ_2 and γ_3) depend on temperature.

By assuming that the kinetic is described by first order laws for the four reactions, the mass balance of the solid and slightly volatile components A_1, A_2, A_3, C_2, B and C_3, can be respectively written as

$$\frac{dm_{A_1}}{dt} = -k_1 m_{A_1} \quad (5)$$

$$\frac{dm_{A_2}}{dt} = -k_2 m_{A_2} \quad (6)$$

$$\frac{dm_{A_3}}{dt} = -k_3 m_{A_3} \quad (7)$$

$$\frac{dm_{C_2}}{dt} = \gamma_2 k_2 m_{A_2} \quad (8)$$

$$\frac{dm_B}{dt} = k_3 \beta m_{A_3} - k_4 m_B \quad (9)$$

$$\frac{dm_{C_3}}{dt} = \gamma_3 k_4 m_B \quad (10)$$

where k_1, k_2, k_3 and k_4 are the rate constants of reactions (1), (2), (3) and (4), respectively, and m_{A_1}, m_{A_2}, m_{A_3}, m_{C_2}, m_B and m_{C_3}represent the mass of the constituents A_1, A_2, A_3, C_2, B and C_3, respectively. Here, $m(t)$ represents the total mass of the sample at the time t, which is

$$m(t) = m_{A_1}(t) + m_{A_2}(t) + m_{A_3}(t) + m_{C_2}(t) + m_{C_3}(t) + m_B(t) \quad (11)$$

The analytical resolution of the balance equations leads to the following equation:

$$\left(\frac{m(t)}{m_{A_0}}\right) = \alpha_2\gamma_2 + \alpha_3\gamma_3\beta + \alpha_1 \times \exp(-k_1 t) + \alpha_2(1-\gamma_2) \times \exp(-k_2 t) + \alpha_3\left(1 - \left(\frac{\beta k_3}{k_3 - k_4}\right) + \left(\frac{\beta\gamma_3 k_4}{k_3 - k_4}\right)\right) \times \exp(-k_3 t) + \left(\frac{\alpha_3\beta k_3}{k_3 - k_4}\right)(1-\gamma_3) \times \exp(-k_4 t) \quad (12)$$

where $m_{A_0}$is the mass of the dried wooden powder at 423 K.

3.1. Determination of the model parameters

Eq. (12) shows that the mass of the sample during the pyrolysis at fixed temperature in an inert atmosphere depends on 10 parameters (α_1, α_2, α_3, γ_2, γ_3, β, k_1, k_2, k_3 and k_4). From the experimental curves, it is not possible to determine all these parameters without carrying out a sequential analysis. Based on the experimental mass loss rate (Fig. 2) beyond 550 K, we can observe that the third peak of the mass degradation rate is more intense than the first two. This indicates that the mass fraction α_3 of A_3 is higher than ($\alpha_1 + \alpha_2$) of the pseudo-components A_1 and A_2. The same experimental results show that the fraction α_2 of A_2 is higher than α_1 of A_1. After several test simulations of the mass loss evolution, we have fixed the sum of the mass fractions of the pseudo-components A_1 and A_2 to 0.4 ($\alpha_1 + \alpha_2 = 0.4$) and the mass fraction of A_3 to 0.6 ($\alpha_3 = 0.6$). These values of $\alpha_1 + \alpha_2$ and α_3 conform to the best description of the experimental evolution of the mass loss.

The degradation of the three pseudo-components A_1, A_2 and A_3 of the olive wood occurs in different temperature ranges. At low temperature (498 K $\leq T \leq$ 523 K), the number of unknown parameters is limited to two (k_1 and k_2) and to four parameters (k_3, k_4, β and γ_3) at high temperatures (598 K $\leq T \leq$ 648 K). For

the intermediate temperatures (523 K ≤ T ≤ 598 K), we determine the values of the parameters k_2, k_3, β and γ_3, and keep the same value of γ_2 and extrapolate the expressions of k_1 and k_4. This semi empirical procedure is certainly not the best, but its merit is that it does not require a simultaneous determination of the all parameters. Then, we consider the three following domains:

- at low temperatures (498 K ≤ T ≤ 523 K), only reactions (1) and (2) take place. In this case, $m(t)$ can be written as

$$\left(\frac{m(t)}{m_{A_0}}\right) = \alpha_2\gamma_2 + \alpha_3 + \alpha_1 \times \exp(-k_1 t) + \alpha_2(1-\gamma_2) \times \exp(-k_2 t) \quad (13)$$

- for high temperatures (598 K ≤ T ≤ 648 K), the decomposition of the olive wood for the two first pseudo-components A_1 and A_2 are total and only the transformation of A_3 remains (reactions (3) and (4)). The variation of the total mass is given by

$$\left(\frac{m(t)}{m_{A_0}}\right) = \alpha_2\gamma_2 + \alpha_3\gamma_3\beta + \alpha_3\left(1 - \left(\frac{\beta k_3}{k_3 - k_4}\right) + \left(\frac{\beta\gamma_3 k_4}{k_3 - k_4}\right)\right) \times \exp(-k_3 t) + \left(\frac{\alpha_3\beta k_3}{k_3 - k_4}\right)(1-\gamma_3) \times \exp(-k_4 t) \quad (14)$$

- between 523 and 598 K, the four reaction stages take place simultaneously and following the assumption proposed, the variation of the total mass is given by

$$\left(\frac{m(t)}{m_{A_0}}\right) = \alpha_2\gamma_2 + \alpha_3\gamma_3\beta + \alpha_1 \times \exp(-k_1 t) + \alpha_2(1-\gamma_2) \times \exp(-k_2 t) + \alpha_3\left(1 - \left(\frac{\beta k_3}{k_3 - k_4}\right) + \left(\frac{\beta\gamma_3 k_4}{k_3 - k_4}\right)\right) \times \exp(-k_3 t) + \left(\frac{\alpha_3\beta k_3}{k_3 - k_4}\right)(1-\gamma_3) \times \exp(-k_4 t) \quad (15)$$

At low temperatures, Eq. (13) can be written for $t \to \infty$ as $m(t)/m_{A_0} = \alpha_2\gamma_2 + \alpha_3 + \alpha_2(1-\gamma_2) \times \exp(-k_2 t)$, because reaction (1) is achieved. At 523 K, the measured residual mass defined by $m_\infty/m_{A_0} = \alpha_2\gamma_2 + \alpha_3$ allows the calculation of the term $\alpha_2 \times \gamma_2$ in Eq. (13) equal to about 0.1 at 523 K. By fitting the slope of the experimental curve $\mathrm{Ln}((m(t)/m_{A_0}) - \alpha_3 - \alpha_2\gamma_2) = -k_2 t + \mathrm{Ln}(\alpha_2(1-\gamma_2))$ for $t \to \infty$ we determine the value of k_2. The values of k_1 and α_1 are obtained by representing at $t \to 0$ the experimental curve $\mathrm{Ln}((m(t)/m_{A_0}) - \alpha_3 - \alpha_2\gamma_2) = -k_1 t + \mathrm{Ln}\alpha_1$ because reaction (2) is not yet released. Then the values of α_1, α_2, k_1, k_2 and γ_2 are obtained. The values of $\alpha_1 = 0.16$ and $\alpha_2 = 0.24$ are used for all temperature ranges of carbonization. These values are in agreement with the amplitudes of the corresponding first and second peaks in Fig. 2. The value of charcoal fraction obtained from A_2 of the wood is equal to $\gamma_2 = 0.42$ assumed constant for $T \geq$ 523 K.

For high temperatures, Fig. 1 shows that the final asymptotic value of the residual mass is about 0.3, taking into account the mass fraction $\alpha_2 \times \gamma_2 = 0.1$ of the non-degradable product (C_2) "charcoal" produced from A_2, the value of the mass fraction of charcoal (C_3) produced from A_3 ($\alpha_3 \times \beta \times \gamma_3$) is equal to 0.2. It can noted here that the fraction of non-degradable product "charcoal" from α_3 was the double of that resulting of α_2 which corresponds appreciably to the identical proportions taking into account the value of $\alpha_2 = 0.24$. The same method used above for low temperature with Eq. (13) is used with Eq. (14) to determine k_3, k_4, γ_3 and β. As shown in Fig. 3, the parameters γ_3 and β are functions of temperature. In fact, the mass fraction γ_3 of the non-degradable solid (C_3) increases to detriment of β

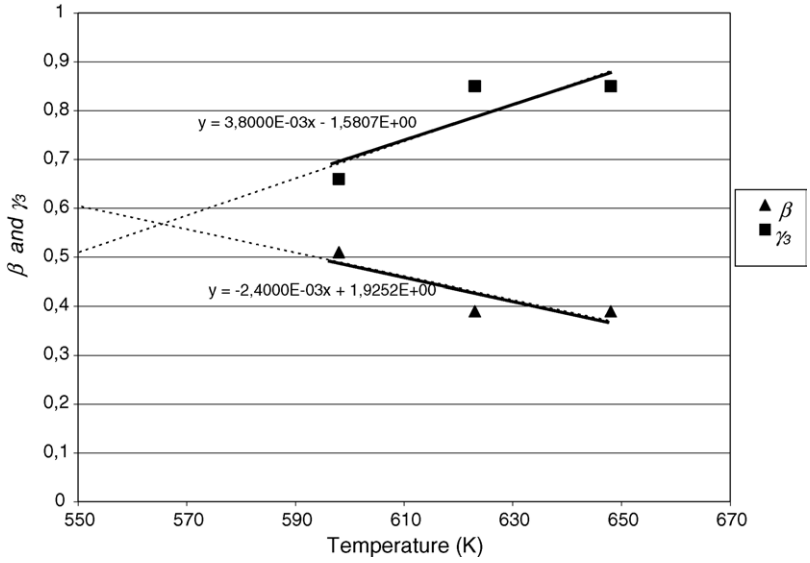

Fig. 3. Variation of the parameters β and γ_3 as function of the temperature.

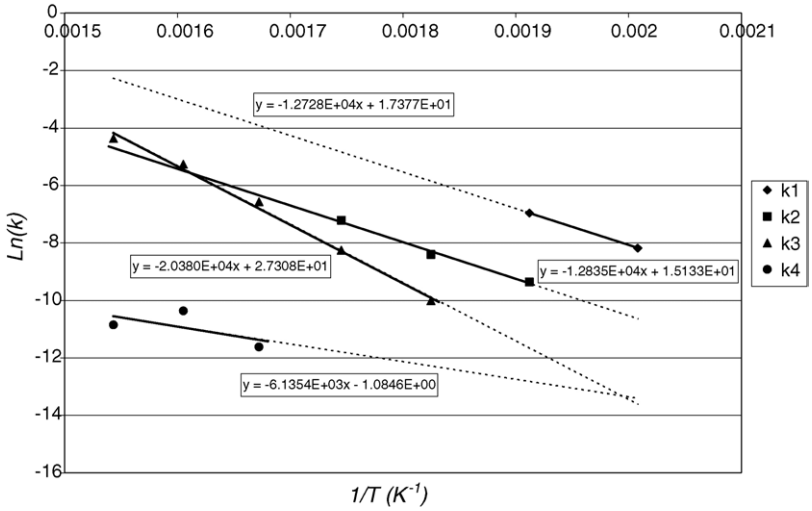

Fig. 4. Arrhenius plot: k_1, k_2, k_3 and k_4 as function of $1/T$.

which represents the mass fraction of the intermediate solid (B) transformed into non-degradable solid "charcoal" (C_3).

By assuming that k_1, k_2, k_3 and k_4 depend on the temperature according to the Arrhenius law, the values of the constants rate k_1 and k_4 are extrapolated in the intermediate range of temperature (Fig. 4).

The experimental curves (Fig. 1) in this range of temperature are used to determine the optimized parameters k_2, k_3, γ_3 and β which depend on temperature. To determine the value of k_2, Eq. (15) can be written for $t \to 0$ as $m(t)/m_{A_0} = 1 - [\alpha_1 k_1 + \alpha_2(1-\gamma_2)k_2]t$ because reactions (3) and (4) have not yet occurred. The values of γ_3 and β are extrapolated in the intermediate range of temperature (Fig. 3). The optimized values of γ_3, β and k_3 can be determined by fitting the experimental and theoretical curves of $m(t)/m_{A_0}$. Indeed, by using the all optimized parameters in the model, the comparison between experimental and calculated curves giving the residual mass according to the time for all the studied temperatures is represented in Fig. 5. By considering the variability of wood, we can deduce that the kinetic model represents accurately all the experimental curves.

All of the optimized values of the model parameters are given in Table 2 in which e is the average relative deviation between the obtained modeling values and the experimental data:

$$e = \left(\frac{1}{N} \sum_{i}^{N} 2 \frac{|m_{\text{cal}} - m_{\text{exp}}|}{m_{\text{cal}} + m_{\text{exp}}} \right) \times 100 \tag{16}$$

The slopes and the origin ordinates of the straight lines of the Arrhenius plot k_i ($i = 1, 2, 3, 4$) reported in Fig. 4 allow the

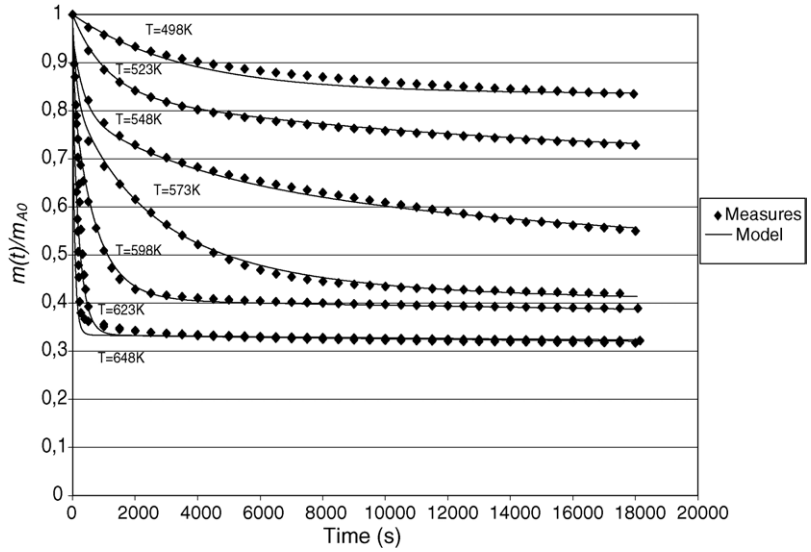

Fig. 5. Verification of the accuracy of model parameters.

Table 2
Kinetic parameters of olive wood carbonization for a temperature range of 498–648 K

T (K)	k_1 (s^{-1})	k_2 (s^{-1})	k_3 (s^{-1})	k_4 (s^{-1})	γ_2	β	γ_3	e (%)
498	2.8×10^{-4}	2.4×10^{-5}	1.22×10^{-6}	1.5×10^{-6}	0.95	–	–	1.00
523	9.5×10^{-4}	8.65×10^{-5}	8.63×10^{-6}	2.71×10^{-6}	0.42	–	–	0.12
548	2.9×10^{-3}	2.25×10^{-4}	4.5×10^{-5}	4.64×10^{-6}	0.42	0.66	0.5	1.00
573	7.94×10^{-2}	7.4×10^{-4}	2.6×10^{-4}	7.56×10^{-6}	0.42	0.54	0.62	1.00
598	2×10^{-2}	1.8×10^{-3}	1.4×10^{-3}	9×10^{-6}	0.42	0.51	0.66	0.60
623	$4.72. \times 10^{-2}$	4.21×10^{-3}	5.2×10^{-3}	3.16×10^{-5}	0.42	0.391	0.85	0.90
648	1.04×10^{-1}	9.34×10^{-3}	1.27×10^{-2}	1.95×10^{-5}	0.42	0.39	0.85	1.00

Table 3
Kinetic constants of the four reactions

Reactions	E_a (kJ mol^{-1})	k_0 (s^{-1})
(1)	105.89	3.5×10^{7}
(2)	106.78	3.72×10^{6}
(3)	169.56	7.23×10^{11}
(4)	51.04	3.4×10^{-1}

activation energies E_{a_i} and the pre-exponential factors k_{0i} of the global reactions to be respectively estimated (Table 3).

3.2. Model validation

Here we propose a comparison of the obtained values of the activation energies E_{a_i} with those available in the literature. Overall the comparisons with literature results can be considered good, taking into account the differences in the experimental technique (isothermal versus dynamic thermogravimetry), the feedstock properties/characteristics, the reaction temperatures, the mathematical treatment of the data and the kinetic mechanisms [8]. Indeed, for the first reaction (or the first pseudo-component A_1), typical activation energies are of the order of 84–140 kJ mol^{-1} [1,17–20], against a value of 106 kJ mol^{-1} estimated here. Activation energies for the second reaction are reported to vary between 73 and 121 kJ mol^{-1} [1,17–20] against a value of 107 kJ mol^{-1} estimated here. For the third reaction, the activation energy is of the order of 170 kJ mol^{-1} which is relatively high compared to those available in the literature $112 \leq E_a \leq 133$ kJ mol^{-1} [1,18–20]. The higher value estimated here can be due to the difficulty, for isothermal conditions, to separate the decomposition of the pseudo component A_3 from that of other components (A_2, particularly) [8]. Finally, for the fourth reaction, corresponding to the decomposition of the intermediate solid (B), an activation energy of 51 kJ mol^{-1} is obtained. The lower value estimated here compared to those in the literature (80–108 kJ mol^{-1}) [20,21] can be due to the slow rate of the relative transformation in the studied temperature range (498–643 K) which corresponds to a diffusional transport of a strongly absorbed molecule or an internal rearrangement of chemical structure rich in carbon.

Finally, to facilitate the utilization of our model by other researchers, we propose to represent all our results by the following general analytical equation:

$$\frac{m(t)}{m_{A_0}} = \alpha_2\gamma_2 + \alpha_3\gamma_3\beta + \alpha_1 \times \exp(-k_1 t) + \alpha_2(1-\gamma_2) \times \exp(-k_2 t) + \alpha_3\left(1 - \left(\frac{\beta k_3}{k_3 - k_4}\right) + \left(\frac{\beta\gamma_3 k_4}{k_3 - k_4}\right)\right) \times \exp(-k_3 t) + \left(\frac{\alpha_3\beta k_3}{k_3 - k_4}\right)(1-\gamma_3) \times \exp(-k_4 t) \quad (17)$$

where the values of $\alpha_1 = 0.16$, $\alpha_2 = 0.24$ and $\alpha_3 = 0.6$ are independent of the temperature and $\gamma_2 = 0.42$ at $T \geq 523$ K, k_i (i = 1–4) represents respectively the reaction rate of the four reactions calculated as function of the temperature from the Arrhenius law $k_i = k_{0i}\exp(-E_{a_i}/RT)$, where the values of k_{0i} and E_{a_i} are given in Table 3. The parameters β and γ_3 are given by the following correlations:

$$\beta = -2.4 \times 10^{-3} T + 1.9252 \quad (18)$$

$$\gamma_3 = 3.8 \times 10^{-3} T - 1.5807 \quad (19)$$

4. Conclusion

Global degradation kinetics of olive wood carbonization has been investigated by means of isothermal thermogravimetry. Weight loss has been measured and used to elaborate a two-stage, semi-global multi reaction kinetic model of olive wood carbonization in the temperature range from 473 to 673 K. The isothermal conditions have allowed the kinetic constants (activation energies and pre-exponential factors) to be estimated by means of the analytical solution of the mass conservation equations. Overall the comparisons of the values of the activation energies with literature results can be considered good. Finally, the proposed model is formulated in a general equation given at any time and temperature of the production rate of charcoal (C_2 and C_3), tar (B) and gaseous (G_1–G_4) during wood carbonization. The proposed model will be applied in the next stage to different species of wood sawdust and will be integrated in a complete modeling of carbonization of a thick wood particle.

Acknowledgement

The authors wish to thank the Analysis Central Service of CNRS (Vernaison, France) for realization of the elementary analysis of our Tunisian olive wood.

References

[1] F. Thurner, U. Mann, Ind. Eng. Chem. Process. Des. Dev. 20 (1981) 482.
[2] S.W. Ward, J. Braslaw, Combust. Flame 61 (1985) 261.
[3] B.M. Wagenaar, W. Prins, W.P.M. van Swaaij, Fuel Process. Technol. 36 (1994) 291.
[4] J. Reina, E. Velo, L. Puigjaner, Ind. Eng. Chem. Res. 37 (1998) 4290.
[5] J.N. Barooahm, V.D. Longm, Fuel 55 (1976) 116.
[6] C.A. Koufopanos, G. Maschio, A. Lucchesi, Can. J. Chem. Eng. 67 (1989) 75.
[7] C. Di Blasi, M. Lanzetta, J. Anal. Appl. Pyrol. 40–41 (1997) 287.
[8] C. Branca, C. Di Blasi, J. Anal. Appl. Pyrol. 67 (2003) 207.
[9] C. Di Blasi, Chem. Eng. Sci. 51 (7) (1996) 1121.
[10] K. Halouani et, H. Farhat, Renew. Energy 28 (2003) 129.
[11] A.F. Roberts, Combust. Flame 14 (1970) 261.
[12] M.G. Grönli, Ph.D. Thesis, Norwegian University of Science and Technology, Norway, 1996.
[13] G. Varhegby, M.J. Antal, E. Jakab, P. Szabo, J. Anal. Appl. Pyrol. 42 (1997) 73.
[14] J.J.M. Orfao, F.J.A. Antunes, J.L. Figueiredo, Fuel 78 (1999) 349.
[15] L. Helsen, E. Van den Bulck, J. Anal. Appl. Pyrol. 53 (2000) 51.
[16] M.J. Antal, G. Varhegby, Ind. Eng. Chem. Res. 34 (1995) 703.
[17] R. Bibao, J.F. Mastral, M.E. Aldea, J. Ceamos, J. Anal. Appl. Pyrol. 42 (1997) 189.
[18] W.-C.R. Chan, M. Kelbon, B. Krieger, Fuel 64 (1985) 1505.
[19] R. Front, A. Marcilla, E. Verdu, J. Devessa, Ind. Eng. Chem. Res. 29 (1990) 1846.
[20] M.G. Grönli, M.C. Melaaen, Energy Fuels 14 (2000) 791.
[21] A.G. Liden, F. Berruti, D.S. Sott, Chem. Eng. Commun. 65 (1988) 207.